Facile method for detecting $C_{23}H_{25}ClN_2$ in fish using Au nanoparticle films as SERS substrates on glass

Yan-meng Li, Li-wei Wang, Ruo-ping Li ✉, *Jun-he Han, Ming-ju Huang*

Key Laboratory of Informational Opto-Electronical Materials and Apparatus, School of Physics and Electronics, Henan University, Kaifeng 475004, People's Republic of China
✉ *E-mail: lrpmm@henu.edu.cn*

Published in Micro & Nano Letters; Received on 4th January 2018; Revised on 27th February 2018; Accepted on 9th March 2018

Malachite green ($C_{23}H_{25}ClN_2$) is an illegal fungicide of aquatic products due to its potential carcinogenic, teratogenic, and mutagenic effects. It is typically challenging to detect $C_{23}H_{25}ClN_2$ in fish with conventional techniques. The study reported a simple and rapid method for detecting $C_{23}H_{25}ClN_2$ on fish surface with surface-enhanced Raman scattering (SERS). Using the seed growth method with trometamol as the modifier, 110 nm in-diameter gold nanoparticles on thin glass as SERS substrate were prepared, which exhibited high SERS activity, reproducibility, stability, and flexibility in SERS measurement. The fish samples required no pretreatment and the entire measurement took <5 min. Quantitative analyses were also conducted. Excellent linear relationships ($R^2 = 0.9397$–0.9977) were obtained between the concentrations and the peak intensities of $C_{23}H_{25}ClN_2$ at some characteristic peaks with a wide concentrations range (0.5–10 μM). The detection limit can reach 0.5 μM. This method provided an easy and fast way to detect $C_{23}H_{25}ClN_2$ on fish surface for food safety.

1. Introduction: Malachite green ($C_{23}H_{25}ClN_2$) a cationic triphenylmethane organic dye [1], was once introduced in aquaculture as a cheap fungicide, ectoparasiticide, and medical disinfectant [2]. However, it has been banned for use in edible animals, because $C_{23}H_{25}ClN_2$ possesses potential carcinogenic, teratogenic, and mutagenic effects [3]. Nevertheless, $C_{23}H_{25}ClN_2$ is still being applied illegally, especially in aquaculture due to its excellent bactericidal effect and low price. Many techniques have been tested to detect $C_{23}H_{25}ClN_2$ in fish such as electrochemiluminescence [4], liquid chromatography tandem mass spectrometry [5], high-performance liquid chromatograph [6], and fluorescence [7]. These above techniques usually require expensive instruments and time-consuming sample pretreatment, whereas cannot provide accurate quantitative measurement. The main challenge is that some complex ingredients in fish such as fat, protein, inorganic salt, and macromolecular, which are difficult to filter, and therefore interfere with the qualitative and quantitative detections of $C_{23}H_{25}ClN_2$. As a result, a simple, quick, and sensitive method for detecting $C_{23}H_{25}ClN_2$ in fish is urgently needed.

Surface-enhanced Raman scattering (SERS) Spectroscopy is a powerful vibrational spectroscopy technique that allows highly sensitive structural detection of low-concentration analytes [8]. SERS as a powerful analytical tool is widely used in catalysis [9], sensing [10], single molecule detection [11], food safety [12, 13], trace fraction analysis [14], and DNA research [15]. The electromagnetic fields enhancement is considered to be the major enhancement reason for SERS [16, 17]. It is derived from the localised surface plasmon resonance (LSPR) effect of metal nanostructures in the electromagnetic field [18, 19]. Long-term studies have found that only few metals [such as gold (Au), silver (Ag), and copper] microstructures or nanostructures can produce SERS enhancement effect. It has also been found that though the chemical composition and chemical properties of Au and Ag are different, they can produce similar plasma oscillation effect and corresponding electromagnetic enhancement effect in the long wavelength region [20]. In general, Au nanoparticles are much more stable than Ag nanoparticles, and also demonstrate excellent sensitivity [21] and provide substantial enhancement of Raman scattering signals for many compounds such as $C_{23}H_{25}ClN_2$. Tian *et al.* reported that the maximum 'hot sites' are at the junction of two nanoparticles in all cases [22], and the enhancement value keeps on increasing with the increase of Au particle sizes until about 110 nm, when the strong radiation damping causes significant reduction of the field enhancement, which results in reduced Raman activity.

Reproducible quantitative detection of trace molecules is another challenge faced by SERS measurement. Raman signal depends on not only the species, shape, size, and density of the materials, but also the relative position of analyte molecules [23], which can affect SERS signal strength significantly. Therefore, quantitative measurement using SERS technology requires uniform, stable, and repeatable SERS substrates. However, it is difficult to use some traditional preparation methods [such as the sodium citrate ($C_6H_5Na_3O_7$) reduction method] to synthesise Au nanoparticles with uniform shapes and sizes.

In this work, we prepared 110 nm Au nanoparticle monolayer films with uniform shape and size and used them as SERS substrates to detect $C_{23}H_{25}ClN_2$ on fish surface. This method does not require complicated and time-consuming sample pretreatment, and the preparation of SERS substrates is easy. In addition, the signal intensities for $C_{23}H_{25}ClN_2$ were reproducible before and after washing fish samples with water. The experimental data demonstrated strong linear relationships between Raman peak intensities and concentrations of $C_{23}H_{25}ClN_2$. Furthermore, quantitative detection with this method can be realised within a wide range of $C_{23}H_{25}ClN_2$ concentration on fish surface.

2. Experimental section

2.1. Chemicals and reagents: Chloroauric acid ($HAuCl_4$, ≥99%), $C_6H_5Na_3O_7$ (99%), trometamol (≥99.9%), and $C_{23}H_{25}ClN_2$ (>99%) were purchased from Aladdin. Hydrogen peroxide (H_2O_2, 30%), ethanol (C_2H_6O, ≥99.7 wt%), and cyclohexane solution (C_6H_{12}, ≥99.5 wt%) were obtained from Kaifeng Reagent Factory in China. The fish samples came from a local market. All solutions were diluted by water, and the water used in the whole study was Milli-Q water (≥18.25 MΩ cm).

2.2. Synthesis of SERS active Au nanoparticles: Au nanoparticles were prepared by the seed growth method with tromethamine as the modifier. Au seeds with 15 nm diameter were prepared using the method reported by Frens [24]. An aqueous solution of

doi: 10.1049/mnl.2017.0911

$HAuCl_4$ (50 ml, 0.01 wt%) was heated to boiling, followed by the rapid addition of $C_6H_5Na_3O_7$ solution (0.5 ml, 1 wt%). The colour of the boiling solution changed from yellow to red wine after 15 min. Then, the colloid was cooled to room temperature and centrifuged at 8000 rpm for 5 min to recover the original concentration for purification.

Synthesis of 110 nm Au nanoparticles: Sequentially 100 µl tromethamine solution (0.1 M), 50 µl Au seed colloid, and 100 µl $HAuCl_4$ solution (1 wt%) were dropped into a 50 ml round bottom flask. After 1 min, 100 µl H_2O_2 (30%) was added into the mixed liquid under strong stirring for 15 min. The above synthesis was carried out at room temperature. The solution colour changed from red wine to jacinth in 30 s.

2.3. Preparation of Au nanoparticle SERS substrates: *Preparation of Au nanoparticle monolayer films*: 5 ml C_6H_{12} was added into 20 ml Au nanoparticle solution. Subsequently, 5 ml C_2H_6O was added into the Au nanoparticle solution drop by drop, the Au nanoparticles soon rose on the interface of water and cyclohexane, and they self-assembled as a dense monolayer. Then, the monolayer films were extracted with clean glass sheets and dried at 80°C for 15 min.

2.4. Pretreatment of fish samples: Six petty fishes were placed in six 500 ml beakers containing 400 ml water. The $C_{23}H_{25}ClN_2$ solutions with different concentrations (0, 0.5, 1, 2, 5, and 10 µM) were added to the six beakers, respectively. Then, the six fishes were raised for a week for further experiments.

2.5. SERS measurement: Raman spectra of samples were recorded using a confocal Raman spectrometer (Renishaw, RM-1000, England) with 633 nm, 20 mW helium–neon laser for Raman excitation, and the acquisition time was 10 s. Raman source with a 633 nm wavelength helps enhance the LSPR effect of Au nanoparticles, and thus obtain stronger resonance Raman signal of $C_{23}H_{25}ClN_2$.

Fish samples were taken out from $C_{23}H_{25}ClN_2$ solutions and placed on sample table. Just as shown in Fig. 1*a*, the monolayer films prepared on thin glass were put on the fish surface to detect the Raman signals, which the Au nanoparticles clung to the fish surface.

3. Results and discussion

3.1. Characteristics of Au nanoparticles: Here, the 110 nm spherical Au nanoparticles were prepared by the seed growth method modified with tromethamine. Fig. 2*a* shows the morphology image of the Au nanoparticle monolayer film scanned by the field-emission scanning electron microscope (FE-SEM; JEOL, JSM-7001F, Japan). It can be seen from Fig. 2*a* that the Au nanoparticles on the glass were all spherical particles with almost same size and their average diameter was about 110 nm. To further confirm their size and their uniformity, the probability diagram of their diameters detected by dynamic light scattering (DLS) was shown in Fig. 2*b*, in which 110 ± 8 nm is the maximum probability. The absorption spectra of Au nanoparticle colloidal solution and $C_{23}H_{25}ClN_2$ aqueous solution in visible light range were shown in Fig. 2*c* using a ultraviolet–visible (UV–vis) absorption spectrometer. The plasma resonance absorption peak of Au nanoparticle solution is near 570 nm, and that of the $C_{23}H_{25}ClN_2$ aqueous solution is near 617 nm.

3.2. SERS analysis of $C_{23}H_{25}ClN_2$ in standard solution and fish samples: The conventional Raman spectra of $C_{23}H_{25}ClN_2$ powder was shown in Fig. 3*a*. The prominent peaks of $C_{23}H_{25}ClN_2$ are attributed to phenyl-C-phenyl out-of-plane bending (438 cm^{-1}), ring C–H out-of-plane bending (798 and 916 cm^{-1}), ring C–H in-plane bending (1174 cm^{-1}), N-phenyl stretching (1365 cm^{-1}), and ring C–C stretching (1613 cm^{-1}) [25]. The monolayer films of Au nanoparticles on the glass were soaked in $C_{23}H_{25}ClN_2$ aqueous solution with different concentrations (0.5, 1, 2, 5, and 10 µM) for 24 h, and then dried. In virtue of the electrostatic attractive force, the cationic $C_{23}H_{25}ClN_2$ molecules can adsorb tightly on the surface of the Au nanoparticles encapsulated by citrate radicals. The Raman spectra of $C_{23}H_{25}ClN_2$ standard

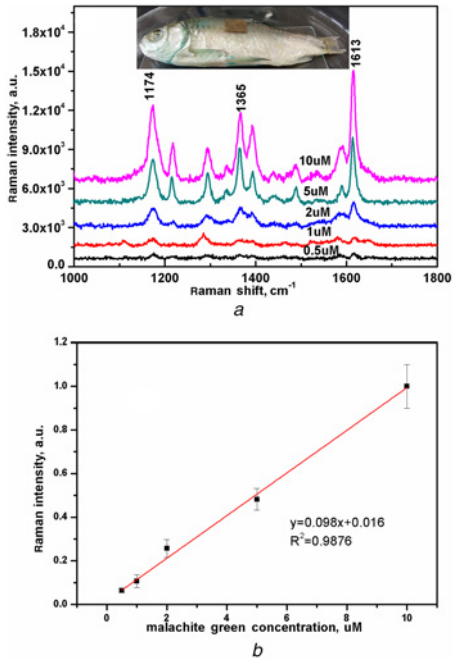

Fig. 1 *Samples and the results of the Raman detection on fish surface*
a Raman spectrum of the $C_{23}H_{25}ClN_2$ on fish surfaces
b Linear relationship between $C_{23}H_{25}ClN_2$ concentrations and Raman intensities of the band at 1174 cm^{-1} after washing fish for 1–5 times

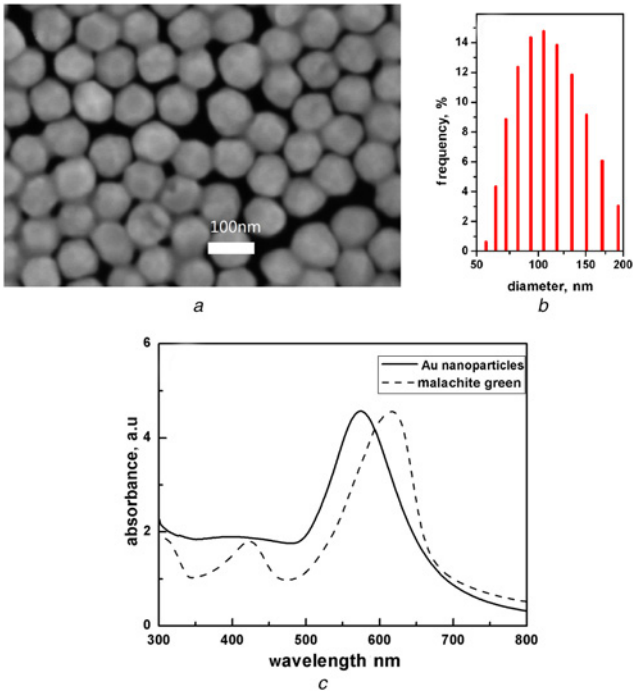

Fig. 2 *Morphology and UV–vis spectra of the Au nanoparticles*
a SEM image of the Au monolayer film on a thin glass surface
b Probability distribution of Au nanoparticle diameter detected by DLS
c UV–vis spectra of Au nanoparticle colloid and $C_{23}H_{25}ClN_2$ solution

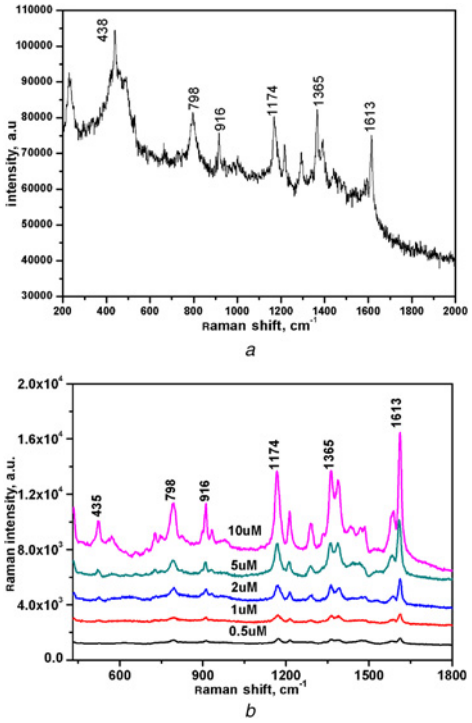

Fig. 3 *Raman spectra of $C_{23}H_{25}ClN_2$*
a Traditional Raman spectra of $C_{23}H_{25}ClN_2$ powder
b SERS spectra of $C_{23}H_{25}ClN_2$ aqueous solution with different concentrations

aqueous solutions with various concentrations (0.5, 1, 2, 5, and 10 μM) enhanced by Au nanoparticle monolayer film were shown in Fig. 3*b*.

In the confocal Raman microRaman system, the SERS enhancement factor (EF) is calculated [26] by experiment

$$\mathrm{EF} = \frac{I_{\mathrm{surf}}}{I_{\mathrm{bulk}}} \times \frac{hcN_{\mathrm{A}}\sigma}{R}$$

where I_{surf} is the surface-enhanced Raman intensity, I_{bulk} is the normal Raman intensity, R is the surface roughness factor at the base of the light, σ is the surface accumulation of a single probe molecule that is about 1.6 nm^2, h is the effective height within the scattered volume that is 222 μm, c is the concentration of the probe molecule that is 10 μM, N_{A} is Avogadro constant. The EF of the three-dimensional structure is about 5.34×10^6 by calculation.

Linear relationships between Raman intensities and $C_{23}H_{25}ClN_2$ concentrations were also obtained. Table 1 demonstrated that there are linear relationships ($R^2 = 0.9397$–0.9977) between $C_{23}H_{25}ClN_2$ concentrations and corresponding Raman intensities for each of the six major characteristic peaks. Fig. 4 displayed that the best linear

Table 1 Linear relationships between $C_{23}H_{25}ClN_2$ concentrations (0.5–10 μM) and SERS intensities at characteristic peaks of $C_{23}H_{25}ClN_2$

Peaks, cm^{-1}	Linear function	R^2
1613	$y = 0.088x - 0.004$	0.9397
1365	$y = 0.087x - 0.070$	0.9507
1174	$y = 0.096x + 0.024$	0.9977
916	$y = 0.091x + 0.068$	0.9778
798	$y = 0.084x + 0.059$	0.9608
435	$y = 0.103x + 0.001$	0.9922

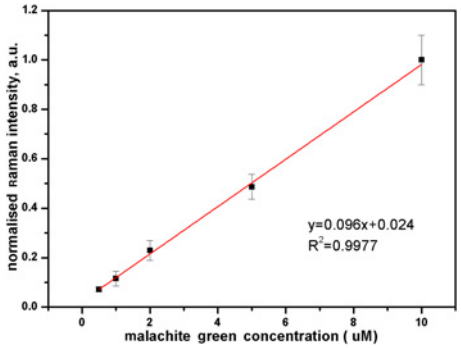

Fig. 4 *Linear relationship between $C_{23}H_{25}ClN_2$ concentrations and normalised Raman intensities of the band at 1174 cm^{-1}*

Table 2 Recovery of $C_{23}H_{25}ClN_2$ from treated fish sample

Concentration of $C_{23}H_{25}ClN_2$ in treated fish, μM	Average Raman peak intensity, au	Amount found[a], μM	Mean recovery, %	RSD[b], %
0.5	9590	0.461	92.2	6.5
1	16171	0.929	92.9	5.7
2	30,723	1.963	98.1	6.0
5	72,728	4.948	98.9	5.3
10	137,638	9.560	95.6	5.1

[a]Average value from ten determinations for each concentration.
[b]Relative standard deviation of mean recovery [RSD (%) = (SD/mean) × 100]. SD: standard deviation.

relationship ($R^2 = 0.9977$) exists for the 1174 cm^{-1} band. This band represents the ring C–H in-plane bending, and its symmetrical big π bond can be enhanced greatly by Au nanoparticles. Within the optical range used in this Letter, significant electromagnetic enhancements are induced by the LSPR of Au nanoparticles [27]. The most significant enhancement effect is attributed to the molecular resonance of $C_{23}H_{25}ClN_2$, which exhibits a maximum absorption at a wavelength (617 nm) very close to that of the incident laser (633 nm), as was shown in Fig. 2*c*.

To validate the proposed quantification method for use in the field of food analysis, detection of $C_{23}H_{25}ClN_2$ on fish surface by Section 2.5. For the fish sample soaked in 0 μM $C_{23}H_{25}ClN_2$ solution, no $C_{23}H_{25}ClN_2$ signal was detected, and thus it was not included in Fig. 1*a*. In addition, from Table 1 we have learnt that the best linear relationship exists between the intensity of the characteristic peak at 1174 cm^{-1} and various $C_{23}H_{25}ClN_2$ concentrations. Thus, we selected the intensities for the characteristic peak at 1174 cm^{-1} for the recovery rate study. The data were shown in Fig. 1*b* and Table 2. The mean recoveries of $C_{23}H_{25}ClN_2$ and the relative standard deviations are about 92–99% and 5.1–6.5%, respectively. As can be seen from Fig. 1*b*, fish samples were washed 1–5 times with water, and an excellent linear relationship ($R^2 = 0.9876$) still exists between SERS intensity and $C_{23}H_{25}ClN_2$ concentrations. There is still $C_{23}H_{25}ClN_2$ on the fish surface after washing with ultrapure water for 1–5 times, indicating that the $C_{23}H_{25}ClN_2$ is firmly adsorbed on the fish surface. In practise, some impurities on the fish skin could interfere with the Raman signal, resulting in a decrease of signal-to-noise ratio. The recovery data further verified that it is feasible to quantitatively measure $C_{23}H_{25}ClN_2$ on fish surface with this method.

4. Conclusion: A simple and rapid method was presented to detect $C_{23}H_{25}ClN_2$ on fish surface using Au nanoparticle monolayer films on glass as SERS substrates. This substrate

doi: 10.1049/mnl.2017.0911

offers high SERS activity, excellent signal stability, and great signal reproducibility. Linear relationships ($R^2 = 0.9397$–0.9977) between $C_{23}H_{25}ClN_2$ concentrations (0.5–10 μM) and Raman intensities of corresponding characteristic peaks were obtained, and the detection limit can reach 0.5 μM. Fish samples need not be treated, and measurement is very convenient and fast to conduct (<5 min). Moreover, the cost of the involved materials is <0.2 USD per measurement. The Au nanoparticle monolayer films are stable and work well for the detection on the surface of irregular objects. It is anticipated that the reported method can be widely used in food safety and quality analyses.

5. Acknowledgments: This work was sponsored by the National Natural Science Foundation of China (grant nos. 61177004 and U1304617) and the Scientific and Technological Project of Henan Province (grant no. 172102310533).

6 References

[1] Pérez-Estrada L.A., Agüera A., Hernando M.D., *ET AL.*: 'Photodegradation of malachite green under natural sunlight irradiation: kinetic and toxicity of the transformation products', *Chemosphere*, 2008, **70**, p. 2068

[2] Culp S.J., Beland F.A.: 'Malachite green: a toxicological review', *Int. J. Toxicol.*, 1996, **15**, p. 219

[3] Srivastava S., Sinha R., Roy D.: 'Toxicological effects of malachite green', *Aquat. Toxicol. Aquat. Toxicol.*, 2004, **66**, p. 319

[4] Guo Z., Gai P., Hao T., *ET AL.*: 'Determination of malachite green residues in fish using a highly sensitive electrochemiluminescence method combined with molecularly imprinted solid phase extraction', *J. Agric. Food Chem.*, 2011, **59**, pp. 5257–5262

[5] Scherpenisse P., Bergwerff A.A.: 'Determination of residues of malachite green in finfish by liquid chromatography tandem mass spectrometry', *Anal. Chim. Acta*, 2005, **529**, p. 173

[6] Yang J.L, Chen P.J., Li Z.G., *ET AL.*: 'Optimization of HPLC determination of malachite green residue in aquatic products', *South China Fisheries Sci.*, 2010, **6**, (4), pp. 43–49

[7] Mitrowska K., Posyniak A., Zmudzki J.: 'Determination of malachite green and leucomalachite green residues in water using liquid chromatography with visible and fluorescence detection and confirmation by tandem mass spectrometry', *J. Chromatogr. A*, 2008, **1207**, (1–2), pp. 94–100

[8] Sharma B., Frontiera R.R., Henry A.I., *ET AL.*: 'SERS: materials, applications, and the future', *Materials Today*, 2012, **15**, (1–2), pp. 16–25

[9] Kim H., Kosuda K.M., Van Duyne R.P., *ET AL.*: 'Resonance Raman and surface- and tip-enhanced Raman spectroscopy methods to study solid catalysts and heterogeneouscatalytic reactions', *Chem. Soc. Rev.*, 2010, **39**, (12), p. 4820

[10] Qian X., Li J., Nie S.: 'Stimuli-responsive SERS nanoparticles: conformational control of plasmonic coupling and surface Raman enhancement', *J. Am. Chem. Soc.'*, 2009, **131**, (22), pp. 7540–7541

[11] Kneipp K., Wang Y., Kneipp H., *ET AL.*: 'Single molecule detection using surface-enhanced Raman scattering (SERS)', *Phys. Rev. Lett.*, 1997, **78**, (9), p. 1667

[12] Li R., Yang G., Yang J., *ET AL.*: 'Determination of melamine in milk using surface plasma effect of aggregated Au@SiO_2 nanoparticles by SERS technique', *Food Control*, 2016, **68**, pp. 14–19

[13] Yang J.L., Yang Z.W., Zhang Y.J., *ET AL.*: 'Quantitative detection using two-dimension shell-isolated nanoparticle film', *J. Raman Spectrosc.*, 2017, **48**, pp. 919–924

[14] Cecchini M.P., Turek V.A., Paget J., *ET AL.*: 'Self-assembled nanoparticle arrays for multiphase trace analyte detection'. *Nat. Mater.*, 2013, **12**, (2), pp. 165–171

[15] Dougan J.A., Macrae D., Graham D., *ET AL.*: 'DNA detection using enzymatic signal production and SERS', *Chem. Commun.*, 2011, **47**, (16), pp. 4649–4651

[16] Chen C., Hutchison J.A., Clemente F., *ET AL.*: 'Direct evidence of high spatial localization of hot spots in surface-enhanced Raman scattering', *Angew. Chem.*, 2009, **121**, (52), pp. 10116–10119

[17] Merlen A., Lagugnélabarthet F., Harté E.: 'Surface-enhanced Raman and fluorescence spectroscopy of dye molecules deposited on nanostructured gold surfaces', *J. Phys. Chem. C*, 2010, **114**, (30), pp. 12878–12884

[18] Raether H.: 'Surface plasmons on smooth and rough surfaces and on gratings' (Springer, Berlin, Heidelberg, 1988), pp. 1–133

[19] Massarini E., Wästerby P., Landström L., *ET AL.*: 'Methodologies for assessment of limit of detection and limit of identification using surface-enhanced Raman spectroscopy', *Sens. Actuators B, Chem.*, 2015, **207**, (207), pp. 437–446

[20] Etchegoin P.G., Ru E.C.L.: 'Basic electromagnetic theory of SERS', *Angew. Chem., Int. Ed*, 2010, **53**, pp. 1–37

[21] Zheng W., Min Y., Chao C., *ET AL.*: 'Selectable ultrasensitive detection of Hg_2 + with rhodamine 6G-modified nanoporous gold optical sensor'. Sci. Rep., 2016, **6**, p. 29611

[22] Fang P.P., Li J.F., Ren B., *ET AL.*: 'Optimization of SERS activities of gold nanoparticles and gold-core-palladium-shell nanoparticles by controlling size and shell thickness', *Journal of Raman Spectroscopy*, 2008, **39**, (11), pp. 1679–1687

[23] Lu L., Wang H., Zhou Y., *ET AL.*: 'Seed-mediated growth of large, monodisperse core-shell gold-silver nanoparticles with Ag-like optical properties', *Chem. Commun.*, 2002, **2**, (2), p. 144

[24] Frens G.: 'Macmillan company. Controlled nucleation for the regulation of the particle size in monodisperse gold suspensions', *Nature*, 1973, **241**, (105), pp. 20–22

[25] Liang E.J., Ye X.L., Kiefer W.: 'Interaction of halide and halate ions with colloidal silver and their influence on surface-enhanced Raman scattering of pyridine with near-infrared excitation', *Vib. Spectrosc.*, 1997, **15**, (1), pp. 69–78

[26] Popp J., Mayerhöfer T.: 'Surface-enhanced Raman spectroscopy', *Annu. Rev. Anal. Chem.*, 2009, **394**, (7), pp. 1717–1718

[27] Pieczonka N.P.W., Aroca R.F.: 'Cheminform abstract: single molecule analysis by surfaced-enhanced Raman scattering', *Cheminform*, 2008, **39**, (32), p. 946